World Applied Sciences Journal 7 (7): 846-855, 2009
ISSN 1818-4952

Influence of the Geometry on the Numerical Simulation of Isothermal Drying Kinetics of Bananas

[1]*Wilton Pereira da Silva,* [1]*Cleide M.D.P.S. e Silva,* [1]*Pedro L. do Nascimento,*
[2]*Diogo D.P.S. e Silva and* [3]*Cleiton D.P.S. e Silva*

[1]Universidade Federal de Campina Grande, Centro de Ciências e Tecnologia,
Departamento de Física, Campina Grande, PB, Brasil, CEP 58109-970
[2]Universidade Estadual de Campinas (UNICAMP),
Instituto de Matemática, Estatística e Computação Científica,
[3]Instituto Tecnológico de Aeronáutica (ITA), Divisão de Engenharia Eletrônica (IEE)

Abstract: The effect of the geometric representation of bananas on the numerical simulation of its isothermal drying kinetics is studied. To study that effect, it is supposed that the diffusion model describes satisfactorily the drying process with boundary condition of the first type and diffusivity varying as a function of the local moisture content. The geometries used to represent the banana are: infinite cylinder, finite cylinder and ellipsoid. In order to simulate the drying kinetics, the diffusion equation was solved through the finite volume method, with a fully implicit formulation, using cylindrical and generalized coordinates. In the analyses it was used experimental data available in the literature and the expressions for diffusivities were determined through optimization, using inverse method. The best model in the representation of the banana's shape was the ellipsoid but the time demanded in its optimization was about 100 times greater than the time for the infinite cylinder.

Key words: Diffusion . variable diffusivity . finite volume method . cylindrical coordinates . generalized coordinates

INTRODUCTION

In order to describe the thin layer drying kinetics of foodstuffs, using hot air, several authors use liquid diffusion models [1-8]. In many works which use diffusion models, the shape of the solid is approximated to a simple geometry, with the objective of obtaining an analytical solution. In addition, the effective diffusivity is considered constant, as well as the volume of the solid, e.g., the shrinkage is neglected. Naturally, the approximation of the geometry of the solid to a more simple shape (and the other simplifications) introduces an error in the results obtained to describe drying kinetics and in the calculated value for the effective diffusivity.

If the effective diffusivity and the dimensions of the solid are considered constant, the diffusion equation has an analytical solution for several shapes such as sphere, cylinder, slab and ellipsoid, among others. Those solutions can be obtained, for example in [3, 9, 10]. In order to solve the diffusion equation, the simplifications of the shape and shrinkage are made by many authors [1, 4, 5, 8] and in these works it is reported good results to describe drying kinetics in spite of that approximation. But it should be observed that the value obtained for the effective diffusivity is just a parameter which fits the solution of the diffusion equation to the experimental data [11].

For any shape, in general, the diffusion equation must be solved numerically. A method commonly used is the finite volume method, with fully implicit formulation [12]. In Ref. [13] the authors used this method to describe heat and mass transfer inside a single rice kernel during the drying process. In this work, the authors used generalized coordinates due to the irregular shape of the grain and they considered the diffusivity as a constant value.

The discrepancy on the drying kinetics description due to the shape of the solid was studied in [7] using experimental data for rice. The shapes used to approximate the grain's shape were: sphere, finite cylinder and prolate spheroid. In this study the diffusivity was considered constant and that consideration made it possible to use analytical expressions as solutions of the diffusion equation, regarding the boundary condition of the first type, to

Corresponding Author: Dr. Wilton Pereira da Silva, Universidade Federal de Campina Grande, Centro de Ciências e Tecnologia, Departamento de Física, Campina Grande, PB, Brasil, CEP 58109-970

describe the drying process. As expected, the authors found that prolate spheroid represents better the drying kinetics of rice than other considered shapes.

In Ref. [14] it was studied the geometry effect on water diffusivity in prointa-isla verde and broom wheat cultivars. The authors compared the spherical and axissymmetric ellipsoidal geometries applying the finite element method to solve numerically the diffusion equation. In this work, the researchers considered constant diffusivity and boundary condition of the first type.

This paper uses numerical solutions of the diffusion equation to compare isothermal thin layer drying kinetics of banana, using experimental data available in the literature. This will be done considering the following geometric models: infinite cylinder, finite cylinder and ellipsoid. In this comparison, a common restriction to the aforementioned papers is eliminated: the diffusivity is considered as a function of the local moisture content, inside the banana. To accomplish that, the diffusion equation will be solved numerically, for the three geometries, through the finite volume method, using a fully implicit formulation. For all the shapes, the diffusivity will be determined via optimization, using the inverse method.

MATERIALS AND METHODS

The mathematical models for the numerical solution of the diffusion equation presuppose the following hypotheses:

- The mathematical models must be useful to simulate the transport of water or heat inside the solid;
- The solid must be homogeneous and isotropic;
- The spacial distribution of the moisture content (or temperature) must be initially uniform;
- The only mechanism of transport of water (or heat) inside the solid is diffusion;
- The dimensions of the solid can vary during the diffusion;
- The process parameters can vary during the diffusion;
- The surface moisture content (or temperature) of the solid is maintained fixed everywhere during the whole diffusion;

Solution of the diffusion equation: Cylindrical coordinates: In cylindrical coordinates, the diffusion equation for an infinite cylinder (length L_e much greater than the radius R_c) is given in the following way [9, 10]

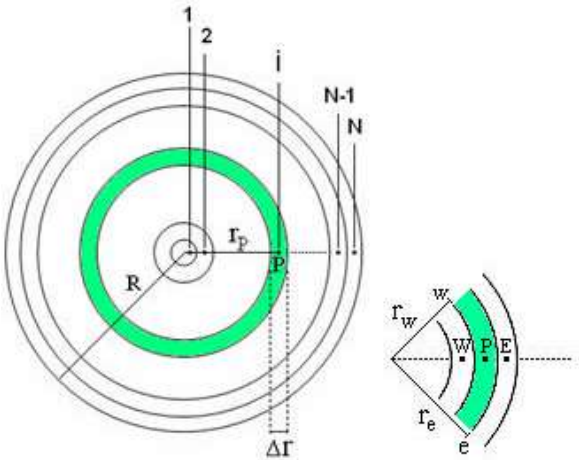

Fig. 1: (a) Uniform mesh: N control volumes with thickness Δr and its nodal points; (b) Control volume P and its neighbors to west (W) and to east (E)

$$\frac{\partial(\lambda.\Phi)}{\partial t} = \frac{1}{r}\frac{\partial}{\partial r}\left(rG^F\frac{\partial F}{\partial r}\right) + S \qquad (1)$$

where Φ is the dependent variable (moisture content or temperature), r defines a position inside the infinite cylinder, λ and Γ^{Φ} are process parameters referring thermophysical properties and S is a source term. In order to discretize Eq. (1), an uniform mesh will be created, with N elements, in the transverse section of the infinite cylinder, as it can be observed in Fig. 1.

The diffusion equation for the model will be solved through the finite volume method [12], with a fully implicit formulation. Integrating Eq. (1) about space ($2\pi r_P \Delta r$) and time (Δt) we obtain the following result for an internal control volume P [8]:

$$A_w F_W + A_p F_p + A_e F_E = B \qquad (2)$$

where,

$$A_W = -\frac{r_w}{\Delta r}G_w^{\Phi};\ A_p = \frac{\lambda_P r_P \Delta r}{\Delta t} + \frac{r_e}{\Delta r}G_e^{\Phi} + \frac{r_w}{\Delta r}G_w^{\Phi} \qquad (3a, b)$$

$$A_e = -\frac{r_e}{\Delta r}G_e^{F};\ B = \frac{\lambda_P^0 r_P \Delta r}{\Delta t}F_P^0 + S_P^{\Phi} r_P \Delta r \qquad (3c, d)$$

where the superscript 0 means "former time" and its absence means "current time". This solution will be used for the description of the drying kinetics of the banana represented by an infinite cylinder. More details

about the numerical solution of the diffusion equation for an infinite cylinder can be obtained in [8].

Solution of the diffusion equation: Generalized coordinates: For a solid with arbitrary shape, the diffusion equation can be solved using structured meshes [15, 16] and generalized coordinates [16, 17]. The diffusion equation in this system of coordinates, presupposing variable thermophysical parameters, can be written in the following way [13, 16, 18]:

$$\frac{\partial}{\partial\tau}\left(\frac{\lambda\Phi}{J}\right)=\frac{\partial}{\partial\xi}\left(\alpha_{11}J\Gamma^{\Phi}\frac{\partial\Phi}{\partial\xi}+\alpha_{12}J\Gamma^{\Phi}\frac{\partial\Phi}{\partial\eta}+\alpha_{13}J\Gamma^{\Phi}\frac{\partial\Phi}{\partial\gamma}\right)+$$
$$+\frac{\partial}{\partial\eta}\left(\alpha_{21}J\Gamma^{\Phi}\frac{\partial\Phi}{\partial\xi}+\alpha_{22}J\Gamma^{\Phi}\frac{\partial\Phi}{\partial\eta}+\alpha_{23}J\Gamma^{\Phi}\frac{\partial\Phi}{\partial\gamma}\right)+ \quad (4)$$
$$+\frac{\partial}{\partial\gamma}\left(\alpha_{31}J\Gamma^{\Phi}\frac{\partial\Phi}{\partial\xi}+\alpha_{32}J\Gamma^{\Phi}\frac{\partial\Phi}{\partial\eta}+\alpha_{33}J\Gamma^{\Phi}\frac{\partial\Phi}{\partial\gamma}\right)+\frac{S}{J}$$

where ξ, η and γ are axes in the generalized coordinates system, τ is time and J is Jacobian of the transformation Cartesian (x,y,z)-generalized (ξ, η, γ) coordinates.

If the solid is obtained by the revolution of a vertical plane area around y axis, Jacobian J is given by the determinant

$$J^{-1}=\begin{vmatrix} x_{\xi} & x_{\eta} & 0 \\ y_{\xi} & y_{\eta} & 0 \\ 0 & 0 & z_{\gamma} \end{vmatrix} \quad (5)$$

In addition, due to the symmetry, terms involving $\partial/\partial\gamma$ are zero and the coefficients α_{11}, α_{22}, α_{12} e α_{21} are given by expressions:

$$\alpha_{11}=z_{\gamma}^{2}\,(x_{\eta}^{2}+y_{\eta}^{2})$$
$$\alpha_{12}=\alpha_{21}=-z_{\gamma}^{2}\,(x_{\xi}x_{\eta}+y_{\xi}y_{\eta}) \quad (6a, c)$$
$$\alpha_{22}=z_{\gamma}^{2}\,(x_{\xi}^{2}+y_{\xi}^{2})$$

In Eqs. (6), the terms of the type "v_u" represent the partial derivative of "v" with respect to "u". On the other hand, a control volume for a solid obtained by revolution of a vertical plane area is shown in Fig. 2.

Again, using the finite volume method, with a fully implicit formulation and integrating Eq. (4) about space and time we obtain the following result for an internal control volume P [18]:

$$A_P\Phi_P=A_W\Phi_W+A_E\Phi_E+A_S\Phi_S+A_N\Phi_N$$
$$+A_{SW}\Phi_{SW}+A_{SE}\Phi_{SE}+A_{NW}\Phi_{NW} \quad (7)$$
$$+A_{NE}\Phi_{NE}+B$$

where,

$$A_P=\frac{\lambda_P}{J_P}\cdot\frac{\Delta\xi\Delta\eta}{\Delta\tau}+\alpha_{11e}J_e\Gamma_e^{\Phi}\frac{\Delta\eta}{\Delta\xi}+\alpha_{11w}J_w\Gamma_w^{\Phi}\frac{\Delta\eta}{\Delta\xi}$$
$$+\alpha_{22n}J_n\Gamma_n^{\Phi}\frac{\Delta\xi}{\Delta\eta}+\alpha_{22s}J_s\Gamma_s^{\Phi}\frac{\Delta\xi}{\Delta\eta}$$

$$A_W=\alpha_{11w}J_w\Gamma_w^{\Phi}\frac{\Delta\eta}{\Delta\xi}+\frac{1}{4}\alpha_{21s}J_s\Gamma_s^{\Phi}-\frac{1}{4}\alpha_{21n}J_n\Gamma_n^{\Phi}$$

$$A_E=\alpha_{11e}J_e\Gamma_e^{\Phi}\frac{\Delta\eta}{\Delta\xi}+\frac{1}{4}\alpha_{21n}J_n\Gamma_n^{\Phi}-\frac{1}{4}\alpha_{21s}J_s\Gamma_s^{\Phi}$$

$$A_S=\alpha_{22s}J_s\Gamma_s^{\Phi}\frac{\Delta\xi}{\Delta\eta}+\frac{1}{4}\alpha_{12w}J_w\Gamma_w^{\Phi}-\frac{1}{4}\alpha_{12e}J_e\Gamma_e^{\Phi}$$

$$A_N=\alpha_{22n}J_n\Gamma_n^{\Phi}\frac{\Delta\xi}{\Delta\eta}+\frac{1}{4}\alpha_{12e}J_e\Gamma_e^{\Phi}-\frac{1}{4}\alpha_{12w}J_w\Gamma_w^{\Phi} \quad (8a\text{-}j)$$

$$A_{SW}=\frac{1}{4}\alpha_{12w}J_w\Gamma_w^{\Phi}+\frac{1}{4}\alpha_{21s}J_s\Gamma_s^{\Phi}$$

$$A_{SE}=-\frac{1}{4}\alpha_{12e}J_e\Gamma_e^{\Phi}-\frac{1}{4}\alpha_{21s}J_s\Gamma_s^{\Phi}$$

$$A_{NW}=-\frac{1}{4}\alpha_{12w}J_w\Gamma_w^{\Phi}-\frac{1}{4}\alpha_{21n}J_n\Gamma_n^{\Phi}$$

$$A_{NE}=\frac{1}{4}\alpha_{12e}J_e\Gamma_e^{\Phi}+\frac{1}{4}\alpha_{21n}J_n\Gamma_n^{\Phi}$$

$$B=\frac{\lambda_P^0\Phi_P^0}{J_P}\cdot\frac{\Delta\xi\Delta\eta}{\Delta\tau}+\frac{S_P}{J_P}\Delta\xi\Delta\eta$$

where the superscript 0 means "former time" and its absence means "current time". So, for each time step, we have a system of equations which will be determined by the Gauss-Seidel method, with tolerance of 10^{-8}. This solution will be used for the description of the drying kinetics of the banana represented by a finite cylinder and an ellipsoid. More details about the numerical solution of the diffusion equation for revolution solids can be obtained in Ref. [18].

Average of Φ: Once Φ is numerically determined in each position and time, the average value at a time t may be calculated by [8, 18, 19]:

$$\overline{F}=\frac{1}{V}\sum_{i=1}^{N}F_iV_i \quad (9)$$

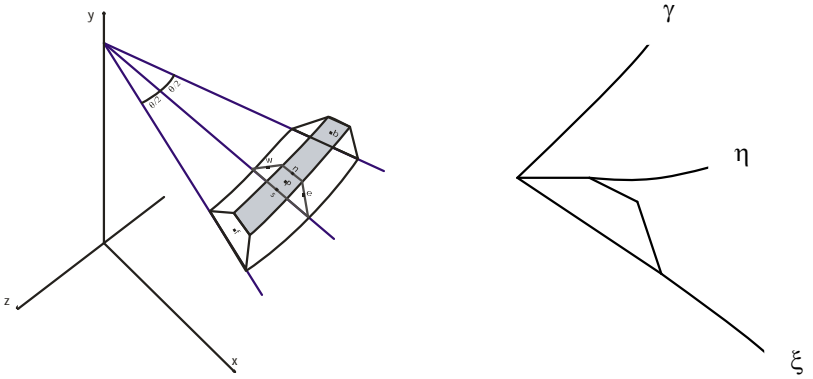

(a) (b)

Fig. 2a: Control volume with a nodal point P obtained by rotation about y of an elementary cell of a two-dimensional structured grid in a vertical plane. The faces "f" and "b" refer to front and back. (b) System of generalized coordinates defined by the axes ξ, η and γ along the borders of the control volume

with

$$V = \sum_{i}^{N} V_i \tag{10}$$

where Φ_i and V_i are the value of Φ and volume of the control volume "i" and N is the number of control volumes.

Parameter Γ^{Φ}: For the nodal points, the process parameter Γ^{Φ} may be calculated from an appropriate relation between such parameter and the local value of the dependent variable Φ,

$$G^{F} = f(F,a,b) \tag{11}$$

where "a" and "b" are parameters which fit the numerical solution to the experimental data and they are determined by optimization.

On the borders of each control volume, for example "e" (between control volumes P and E), the following expression should be used to determine Γ^{Φ} [8, 12]

$$\Gamma_e^{\Phi} = \frac{\Gamma_P^{\Phi}\Gamma_E^{\Phi}}{f_d\Gamma_E^{\Phi} + (1 - f_d)\Gamma_P^{\Phi}} \tag{12}$$

where

$$f_d = \frac{d_P}{d_P + d_E} \tag{13}$$

and d_P e d_E are the distances from the border to the nodal points P and E, respectively.

Optimization: An optimization algorithm using the inverse method was developed considering the following requirements:

minimization of the chi-square regarding the fit process of a curve simulated to the experimental data; use of Levenberg-Marquardt's algorithm [20], with corrections in sequence of the parameters.

The expression for the chi-square regarding the fit of a simulated curve to the experimental data is given by [21]

$$\chi^2 = \sum_{i=1}^{N_p} (\overline{F}\,exp_i - \overline{F}\,sim_i)^2 \frac{1}{s_i^2} \tag{14}$$

where $\overline{F}\,exp_i$ is the experimental value of $\overline{\Phi}$ in the time t_i, $\overline{F}\,sim_i$ is the correspondent simulated value, N_p is the number of experimental data, $1/\sigma_i^2$ is the statistical weight of the experimental point i. In the absence of information, those weights can be made equal to the unit. Obviously, the chi-square depends on $\overline{F}\,sim$ which depends on the process parameter Γ^{Φ}. Generally, Γ^{Φ} can be expressed by a function $f(\Phi,a,b)$ in which "a" and "b" are parameters that can be determined by minimization of χ^2. On the other hand, besides the chi-square which will be used as statistical indicator, the coefficient of determination R^2 [21] will also be utilized to determine the quality of the fit.

Diffusion problems: The proposed numerical solutions can be used to study the conduction of heat if we impose: $\Phi = T$ (temperature), $\Gamma^{\Phi} = k$ (conductivity) and $\lambda = \rho c_p$ (ρ is the density and c_p is the specific heat). On the other hand, establishing $\Phi = M$ (moisture content), $\Gamma^{\Phi} = D$ (water diffusivity), $\lambda = 1$ and $S = 0$ the proposed numerical solution can be used to study the water diffusion in porous solids.

In this article we will use the presented solutions to study the thin layer drying of banana, considered as:

infinite cylinder, finite cylinder and axisymmetric ellipsoid.

Drying of banana: The data presented in Ref. [5] referring to the isothermal thin-layer drying of bananas (radius R_b = 0.0152 m) was used to test the influence of the geometry on the description of the process. The drying happened in the following conditions: air in temperature of 50 °C and relative humidity of 20%. The initial moisture content is 3.21 kg water/kg dry matter and the equilibrium moisture content is 0.0559 kg water/kg dry matter. In their analyses, the authors considered the banana as an infinite cylinder and the model to describe the thin layer drying was the liquid diffusion with boundary condition of the first type. More details can be obtained in [5] and in the references of this paper.

The tests about the influence of the geometry will be done in a computer Intel Pentium IV with 512 MB (RAM). The compilation of the source code will be made in Compaq Visual Fortran (CVF) 6.6.0 Professional Edition, using the programming option QuickWin Application and the platform will be Windows XP. On the other hand, in all the optimization processes, the tolerance on the parameters will be $1.0x10^{-4}$.

RESULTS AND DISCUSSION

Although the proposed numerical solutions in our paper consider dimensional variations, in the presented drying study the shrinkage is ignored because it was ignored in the original article where experimental data is available.

Infinite cylinder: Constant diffusivity: The simulation of the drying kinetics of the banana, presupposing constant diffusivity for the geometry "infinite cylinder", presents a result with the aspect indicated in Fig. 3, which also presents the statistical indicators of the fit and the obtained value for the diffusivity.

Figure 3 and others which will present drying kinetics curves were drawn by software developed for the tests. On the other hand, for the other geometries involved in this study (finite cylinder and ellipsoid), similar results (Fig. 3) are obtained in the description of the experimental data, through numeric simulation, when the diffusivity is considered constant with boundary condition of the first type.

Variable diffusivity: In order to improve the fit of the simulated curve to the experimental data, an observation of Fig. 3 indicates that in the initial instants

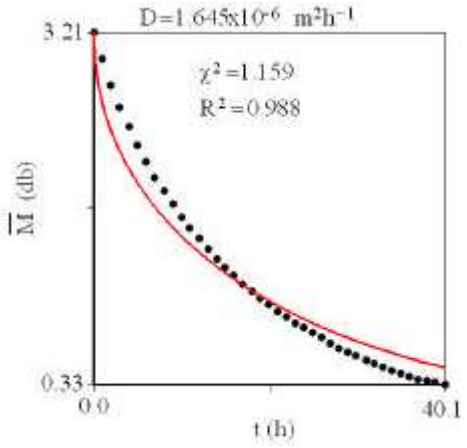

Fig. 3: Drying kinetics of banana, considered as an infinite cylinder with constant diffusivity

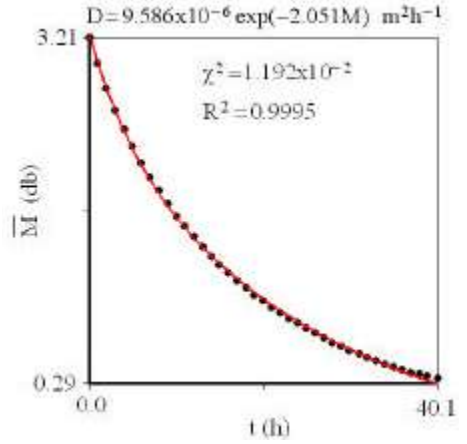

Fig. 4: Drying kinetics of banana, considered as an infinite cylinder with variable diffusivity

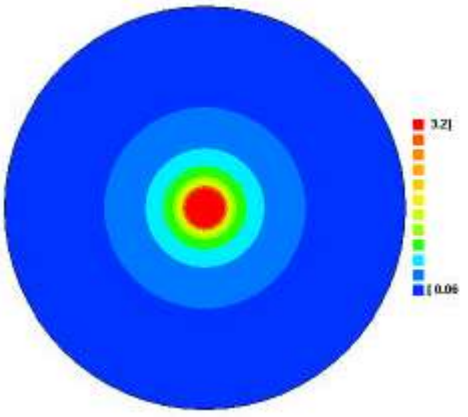

Fig. 5: Contour plot representing the distribution of the moisture content (db) on the transverse section of the banana, considered as an infinite cylinder, in the instant t = 40.1 h

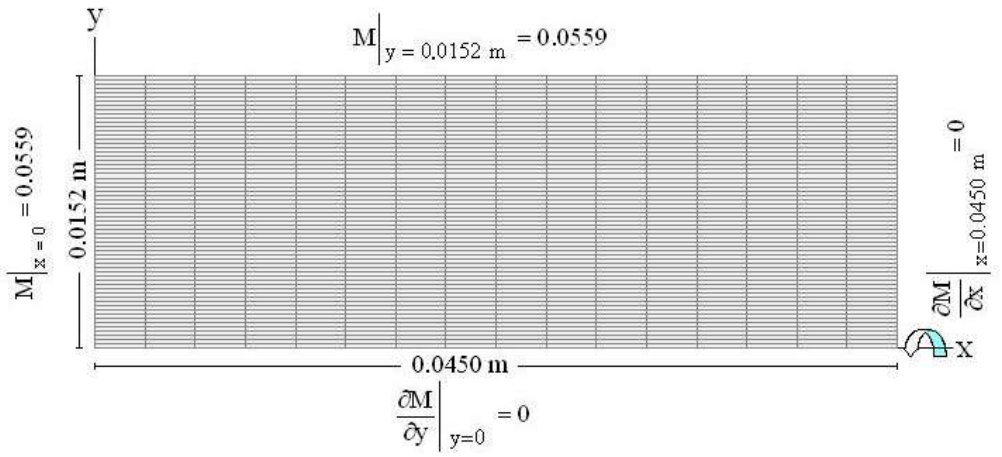

Fig. 6: Rectangular structured mesh 16x64 generating the half cylinder finite which represents the banana: revolution around the axis x

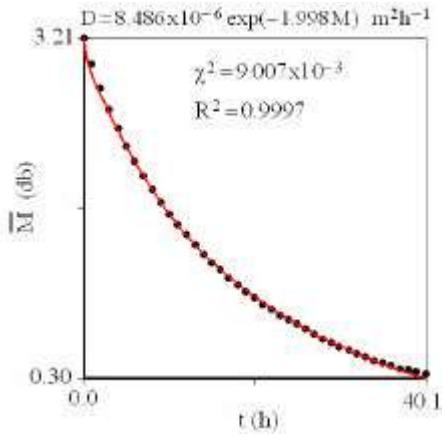

Fig. 7: Drying kinetics of banana, considered as a finite cylinder with variable diffusivity

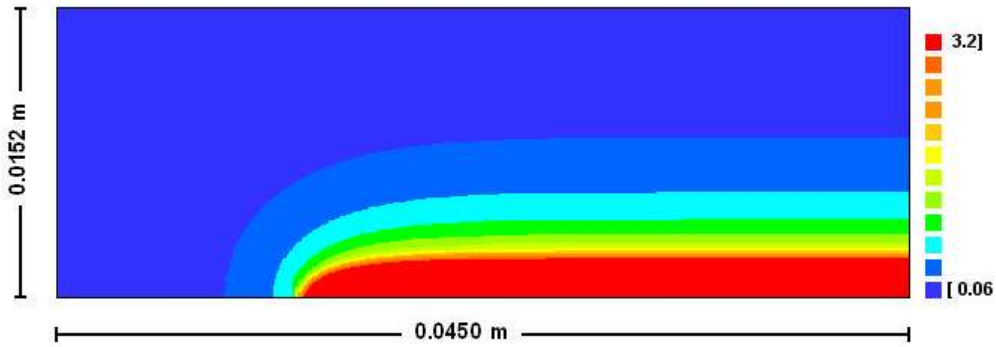

Fig. 8: Contour plot representing the distribution of the moisture content (db) on the quarter-rectangle generating the half finite cylinder which represents the banana, in t = 40.1 h

the diffusivity must be smaller than $1.645x10^{-6}$ m^2h^{-1} and in the final instants it should be larger than this value. Then, admitting that the boundary condition of the first kind is acceptable to describe the drying, it becomes clear that the diffusivity must increase when the moisture content $\overline{M}$ decreases. Establishing, for example, the expression for the diffusivity [22]

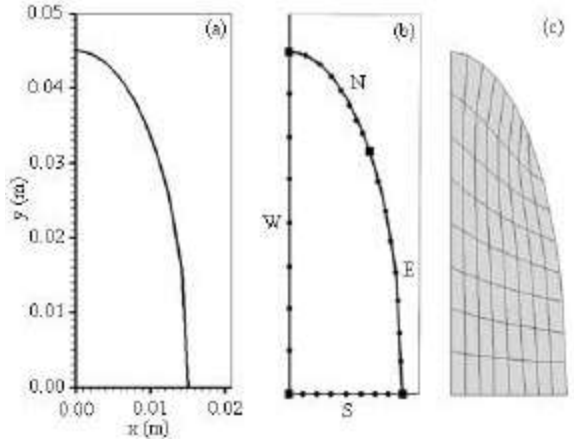

Fig. 9: (a) Graph regarding Eq. (16) which defines the quarter-ellipse generating the ellipsoid; (b) Definition of the points in the boundary for the generation of an initial mesh, showing the boundaries: north (N), south (S) east (E) and West (W); (c) Structured mesh initially generated

$$D = be^{aM} \quad (15)$$

where M is the local moisture content, the parameters "a" and "b" can be determined by optimization, via inverse method.

Obviously, the best way to save time when simulating the drying kinetics for the three geometries is initially to do the optimization for the infinite cylinder, that it is a faster process (one-dimensional) than the others, determining the parameters "a" and "b". Then, the obtained values should be used as initial values for the finite cylinder, that involves an orthogonal structured mesh and that makes the solution of the diffusion equation faster than for the case of a non-orthogonal mesh. Thus, the last obtained values for the parameters should be used as initial values in the solution for the ellipsoidal geometry, which is a slower process, for involving a non-orthogonal structured mesh. However, in order to compare the times of execution of the three simulations, it was established 2000 steps of time for all the geometries and the following values initials for the parameters: a = -1.4 and $b = 4.3\times10^{-6}$ m^2h^{-1}.

Infinite cylinder: The one-dimensional mesh was obtained dividing the transverse section of the infinite cylinder, from r = 0 up to r = 0.0152 m in 64 control volumes. After the optimization process, it is obtained the result shown through Fig. 4, which also shows the expression obtained for the diffusivity and the statistical indicators of the fit.

Naturally, the consideration of variable diffusivity improves the fit of the simulated curve in comparison with constant diffusivity, as it can be observed through the statistical indicators presented in Fig. 3 and 4.

The distribution of the moisture content in the end of the drying process is shown through the contour plot on the transverse section of the infinite cylinder, which can be observed through Fig. 5.

Finite cylinder: The finite cylinder that represents the banana was obtained by the revolution of a rectangle (sides: 0.0152 and 0.045 m) around the axis x, that only represents half the banana, to take advantage of symmetry conditions. The mesh was generated using the software 2D Grid Generation (http://zeus.df.ufcg.edu.br/labfit/gg.htm). The points on the boundary were defined in a file that was read by the software which generated the two-dimensional mesh 16x64 on the quarter-rectangle shown through Fig. 6.

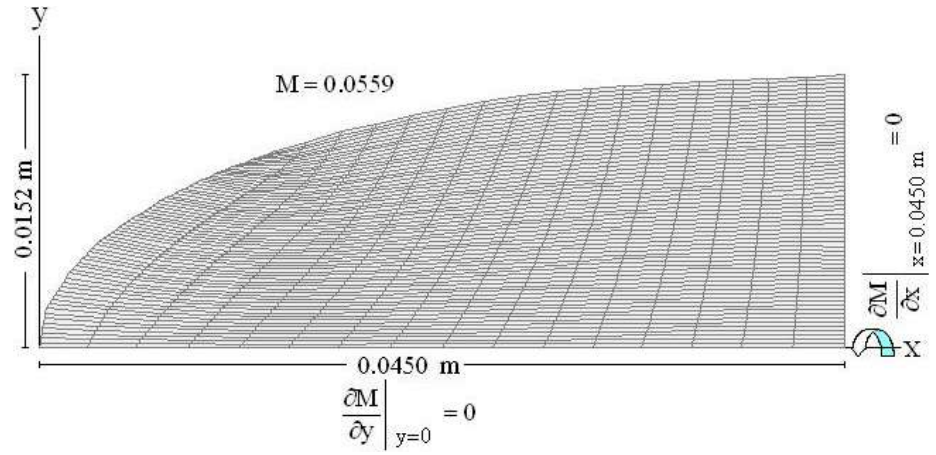

Fig. 10: Structured mesh 16x64 in quarter-ellipse generating the ellipsoid which represents the banana

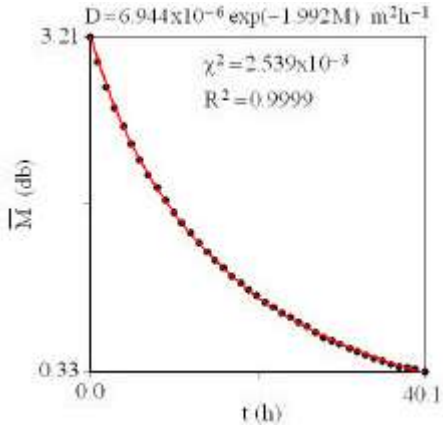

Fig. 11: Drying kinetics of banana, considered as a ellipsoid with variable diffusivity

It should be observed that Fig. 6 indicates the boundary conditions being taken into consideration the symmetry condition that was imposed to the problem. On the other hand, after the optimization process of the numerical simulation to the experimental data, it is obtained the results shown through Fig. 7.

The distribution of the moisture content in the end of the drying process is shown through the contour plot on the quarter-rectangle generating the finite cylinder which represents the banana and it can be observed through Fig. 8.

Ellipsoid: For the dimensions of the banana, the equation of the quarter-ellipse generating the ellipsoid is given by

$$\sqrt{(y-0.04235)^2+x^2}+\sqrt{(y+0.04235)^2+x^2}-0.09=0 \quad (16)$$

Thus, being attributed values for x, it is obtained a transcendental equation that can be solved for the determination of y. In that way, it can be obtained points (x,y) which generates the curve shown in Fig. 9a. If adequate points are chosen in the boundary of the quarter ellipse, like it is shown in Fig. 9b, such figure can be digitized and the structured mesh can be generated through the software 2D Grid Generation (Fig. 9c).

After the refine on the generated initial mesh, it is obtained the structured mesh 16x64 shown through Fig. 10, which is presented with a rotation of 90° counterclockwise with respect to the Fig. 9.

The symmetrical half of the ellipsoid is generated by the revolution of the area around the axis x

As in the case of the finite cylinder, it should be observed that Fig. 10 indicates the boundary conditions being taken into consideration the symmetry condition which was imposed to the problem. On the other hand, after the optimization process it is obtained the results shown through Fig. 11.

Table 1: Summary of the optimization processes for the three geometries

	Diffusivity (m^2h^{-1})	R^2	χ^2
Infinite cylinder	$9.586x10^{-6}$ exp (-2.051M)	0.9995	$1.192x10^{-2}$
Finite cylinder	$8.486x10^{-6}$ exp (-1.998M)	0.9997	$9.007x10^{-3}$
Ellipsoid	$6.944x10^{-6}$ exp (-1.992M)	0.9999	$2.539x10^{-3}$

The distribution of the moisture content in the end of the drying process is shown through the contour plot on the quarter-ellipse generating the ellipsoid and it can be observed through Fig. 12.

Analyses: The results obtained in our article for the three studied geometries can be summarized through Table 1.

Through the results obtained for the three geometries, summarized in Table 1, the behavior of the diffusivities can be observed as function of the local moisture content in Fig. 13.

Through Fig. 13 it can be noticed that, for a given moisture content, the diffusivity is smaller when the considered geometry approximates more of the shape of the banana.

Analyzing the statistical indicators presented in Fig. 4, 7 and 11, it can be noticed that the simulation of the drying kinetics of the banana using an ellipsoidal mesh produces the best results. The worst simulation is that regarding the banana as infinite cylinder, which has a chi-square about five times greater than the chi-square regarding the ellipsoid. However, it should be observed that the optimization process regarding ellipsoidal mesh is about 100 times slower than in the case of the infinite cylinder.

In this article, we use the same boundary condition used in the original paper, from where the data were obtained. Naturally, if the boundary condition of the first kind is not completely acceptable to describe the drying process, the obtained diffusivities should only be interpreted as expressions that fit the numerical simulations to the experimental data. On the other hand, it should be observed that, for the convective boundary condition, in general it is expected that the diffusivities increase with the increasing of the moisture content [11, 23-25] and not the opposite, as the results obtained in this article with boundary condition of the firs kind. Even so, the focused discussion in our article is referring to the influence of the geometry used in the numeric simulation of the drying of banana. In this sense it can be observed through the statistical indicators that, the closer the geometry is to the real

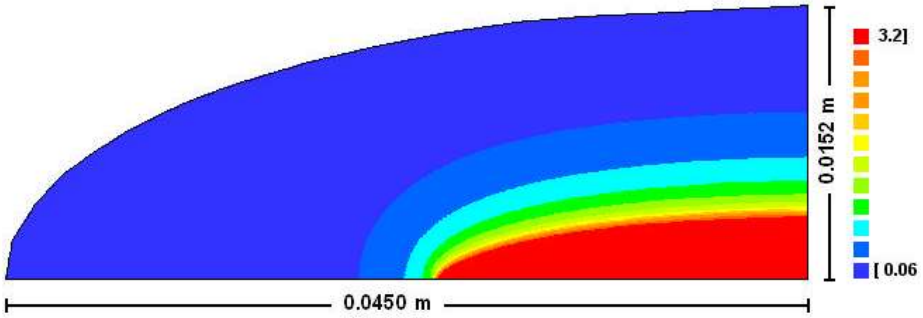

Fig. 12: Contour plot representing the distribution of the moisture content (db) on the quarter-ellipse generating the ellipsoid which represents the banana, in t = 40.1 h

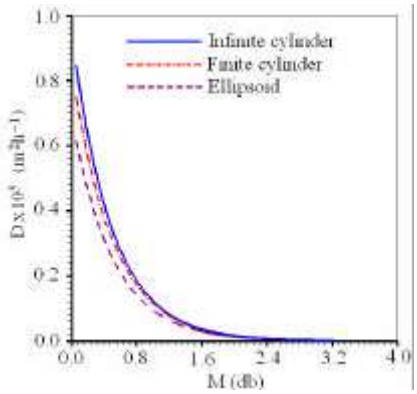

Fig. 13: Dependence of the diffusivity with the local moisture content for the three analyzed geometries

shape of the banana, the better the obtained results are in the description of the drying process.

CONCLUSION

It was observed that the more the shape used in the simulation approximates the shape of the banana, the better are the results obtained for the fit of the curve simulated to the experimental data of the drying kinetics. However, the time demanded in the optimization process of an ellipsoid is substantially larger than the time for the infinite cylinder (about 100 times). Thus, the decision about the geometric model which represents the banana should take into consideration the desired cost-benefit relation in the simulation.

REFERENCES

1. Phoungchandang, S. and J.L. Wodds, 2000. Moisture diffusion and desorption isotherms for banana. Journal of Food Science, 65 (4): 651-657.
2. Gastón, A.L., R.M. Abalone and S.A. Giner, 2002. Wheat drying kinetics. Diffusivities for sphere and ellipsoid by finite elements. Journal of Food Engineering, 52 (1): 313-322.
3. Lima, D.R., S.N. Farias and A.G.B. Lima, 2004. Mass transport in spheroids using the Galerkin method. Brazilian Journal of Chemical Engineering, 21 (1): 667-680.
4. Doymaz, I., 2005. Drying behaviour of green beans. Journal of food Engineering, 65 (10: 161-165.
5. Amendola, M. And M.R. Queiroz, 2007. Mathematical methodologies for calculating the mass diffusion coefficient of bananas during drying. Revista Brasileira de Engenharia Agrícola e Ambiental, 11 (6): 623-627.
6. Resende, O., P.C. Corrêa, C. Jarén and A.J. Moure, 2007. Bean moisture diffusivity and drying kinetics: A comparison of the liquid diffusion model when taking into account and neglecting grain shrinkage. Spanish Journal of Agricultural Research, 5 (1): 51-58.
7. Hacihafizoglu, O., A. Cihan, K. Kahveci and A.G.B. Lima, 2008. A liquid diffusion model for thin-layer drying of rough rice. European Food Research and Technology, 226 (4): 787-793.
8. Silva, W.P., C.M.D.P.S. Silva, D.D.P.S. Silva and C.D.P.S. Silva, 2008. Numerical simulation of the water diffusion in cylindrical solids. International Journal of Food Engineering, 4 (2): Article 6.
9. Luikov, A.V., 1968. Analytical heat diffusion theory. New York: Academic Press.
10. Crank, J., 1992. The mathematics of diffusion. Oxford, UK: Clarendon Press.
11. Ruiz-López, I.I. and M.A. García-Alvarado, 2007. Analytical solution for food-drying kinetics considering shrinkage and variable diffusivity. Journal of Food Engineering, 79: 208-216.

12. Patankar, S.V., 1980. Numerical heat transfer and fluid flow, New York: Hemisphere Publishing Corporation.
13. Wu, B., W. Yang and C. Jia, 2004. A three-dimensional numerical simulation of transient heat and mass transfer inside a single rice kernel during the drying process. Biosystems Engineering, 87 (2): 191-200.
14. Gastón, A.L., R.M. Abalone, S.A. Giner and D.M. Bruce, 2003. Geometry effect on water diffusivity estimation in PROINTA-Isla Verde and broom wheat cultivars. Latin American Applied Research, 33 (3): 327-331.
15. Thompson, J.F., Z.U.A. Warsi and C.W. Mastin, 1985. Numerical grid generation. New York: Elsevier Science Publishing Co.
16. Maliska, C.R., 2004. Transferência de calor e mecânica dos fluidos computacional. LTC Editora S. A., Rio de Janeiro.
17. Tannehill, J.C., D.A. Anderson and R.H. Pletcher, 1997. Computational fluid mechanics and heat transfer. Second Edition, Taylor & Francis, Philadelphia.
18. Silva, W.P., D.D.P.S. e Silva, C.D.P.S. Silva and A.G.B. Lima, 2007. Simulação numérica da transferência de massa em sólidos de revolução via volumes finitos e coordenadas generalizadas. 8º Congresso Iberoamericano de Engenharia Mecânica, Cusco, Peru, 23 a 25 de Outubro.
19. Hadrich, B., N. Boudhrioua and N. Kechaou, 2008. Drying of Tunisian sardine (*Sardinella aurita*) experimental study and three-dimensional transfer modeling of drying kinetics. Journal of Food Engineering, 84: 92-100.
20. Press, W.H., S.A. Teukolsky, W.T. Vetterling and B.P. Flannery, 1996. Numerical Recipes in Fortran 77 The Art of Scientific Computing. New York: Cambridge University Press, Vol: 1.
21. Taylor, J.R., 1997. An introduction to error analysis. Sausalito, California: University Science Books, 2nd Edition.
22. Zogzas, N.P., Z.B. Maroulis and D. Marinos-Kouris, 1996. Moisture diffusivity data compilation in foodstuffs. Drying Technology, 14 (10): 2225-2253.
23. Kiranoudis, C.T., Z.B. Maroulis and D. Marinos-Kouris, 1995. Heat and mass transfer model building in drying with multiresponse data. International Journal of Heat and Mass Transfer, 38 (3): 463-480.
24. Zogzas, N.P. and Z.B. Maroulis, 1996. Effective Moisture diffusivity estimation from drying data: A comparison between various methods of analysis, Drying Technology, 14 (7): 1543-1573.
25. Hamdami, N., J.Y. Monteau and A. Le Bail, 2004. Transport properties of a high porosity model food at above and sub-freezing temperatures. Part 2: Evaluation of the effective moisture diffusivity from drying data. Journal of Food Engineering, 62: 385-392.